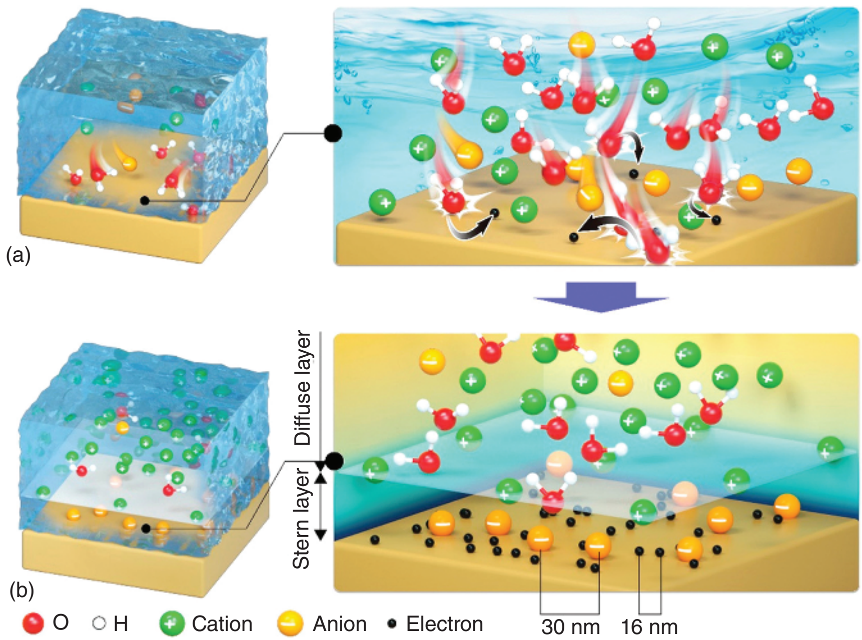

Figure 1.5 The hybrid EDL model with the "two-step" formation process for CE in LSI. (a) The electron transfer in the first step. (b) the EDL formation due to ion migration and redistribution. Source: Reproduced with permission of [44], 2022 © American Chemical Society.

1.5.1 Temperature Effect on the CE

As stated above, high temperature may facilitate the thermionic emission of electrons, as an experimental tool to reveal the CE mechanism, and in the meanwhile, it is also a pathway to release triboelectric charge, which may limit the application scenario of triboelectricity. The TENG used in previous studies is mainly based on CS motions, in which the two triboelectric surfaces are separated mostly. It has been discovered that the charge decay during contact status is much slower than that in separation status, which indicates that more charges can be kept at contact status [11]. Therefore, Wang et al. demonstrated sliding-based CE to generate more charge in high temperatures [59]. It has been discovered that sliding-based CE can facilitate CE charge transfer even in the highest temperature tested. Such a CE mechanism may comprehensively involve surface charge transfer, thermionic emission, and surface contact area changes. Based on sliding CE, Xu et al. developed the preannealing strategy to further raise the working temperature of CE, to be up to 673 K [60]. The mechanism of preannealing strategy to promote charge transfer is attributed to the atomic thermal vibration, which increases with the temperature significantly and partially balances the thermionic emission. Such annealing strategy may even change the polarity of the triboelectric charges in some materials, as carefully examined by KPFM [61]. The annealing strategy may also be unevenly applied on both sides or only on one side, which may facilitate the electron transfer from the heated side to the unheated side, due to thermionic emission of electrons [62]. Such an effect may be used to generate and modify triboelectric charge on purpose, even in identical material pairs, considering the unevenly heated areas in contact surfaces due to frictional heat.

1.5.2 Impact of Material Surface

As an interface effect, the characteristics of CE or triboelectric effect are strongly related to the material surface. The triboelectric series, as the empirical sequence of triboelectric polarity, was usually used to select and compare triboelectric materials qualitatively. Zou et al. developed a quantitative method to understand the triboelectric series by characterizing the triboelectric charge density (TECD) as a material "gene" [63, 64]. In the meanwhile, surface of materials also plays key roles in CE. In the past decade, the method of modifying surface to promote TECD has been intensively investigated, including chemical modification method [65–67] and introduction of surface micro-/nanostructures [68–70]. However, more systematic studies are still required to quantify the promotion effect of surface functional groups.

Li et al. demonstrated that the electron-withdrawing (EW) ability of the functional groups is the key to determining their polarity and resulting TECD [71]. In various functional groups, the −F group shows the best EW ability, and increase of the −F groups can greatly enhance the negative TECD, which explains why polymers that are fully fluorinated (such as FEP and polytetrafluoroethylene, PTFE) demonstrate the best TECD compared to other common polymers. The EW ability for other common functional groups is ranked as $-CH_3 < -H < -OH < -Cl < -F$. Besides, it was discovered that unsaturated groups can enhance the EW of fluorinated polymers, such as $-CF_2{=}CF_2-$ and $-CF{\equiv}CF-$, which may be introduced to the original fluorinated polymers through thin firm sputtering, UV-ozone treatment, etc. In the meanwhile, the density of surface states (DOSS) may also contribute to the resulting TECD [72]. A model based on DOSS was proposed to explain the abnormal TECD generation between ternary materials, with an experimental method established to characterize DOSS of materials. Through this DOSS model, it can be predicted that TECD of FEP may achieve $\sim 560\,\mu C/m^2$, which is close to the reported maximum values. These studies may inspire a more complete mechanism model for CE and TECD in the near future.

1.5.3 Stress/Strain States and Others

Besides the chemical composition of the material surface, the surface stress or strain states may also impact the TECD. However, even for identical material pairs in contact, CE may also happen. Xu et al. demonstrated that the charge transfer is also related to the curvature of surfaces, while positive curvature tends to take negative charge and negative curvature tends to take positive charge [73]. The mechanism of CE between the curved surfaces may be attributed to the shift of occupied level of surface states. In light of that, mutual CE may even happen between any identical material pairs in contact considering the surface roughness, which may result in uneven stress/strain distribution on the surface. This discovery may explain the mosaic distribution of triboelectric charge [22]. Furthermore, the applied stress/strain can also vary the electron transfer amount during CE, which may be contributed by the induced flexoelectricity [74].

For some stretchable polymer materials, the crystallization level may be induced by strain, which can greatly impact the band diagram. Liu et al. demonstrated that strain-induced crystallization can shift the position of polymers in triboelectric series, and even induce polarity reversal of TECD [75]. With the crystallization process, the electron cloud on the surface can be totally redistributed, which can greatly impact the CE process by assuming the electron-dominated electron-cloud-potential-well model. CE can also be promoted by UV light, as attributed to photoexcitation effect on electrons [15, 76], which demonstrated the existence of threshold photon energy to assist electrons to overcome the potential barrier heights. The TECD can even be modified by atmosphere, especially the oxygen atmosphere, which may both impact the DOSS and occupied energy levels [77].

1.6 Potential Applications

When two different materials or surfaces are in physical contact or sliding against one another, charges will be transferred from one surface to the other, making them positively or negatively charged, respectively. This is the triboelectric effect (also called triboelectrification or CE) well-known for thousands of years, which was first recorded by Thales of Miletus (c. 624–546 BC), an ancient Greek philosopher. Understanding and discovering methods to tailor the triboelectric effect by controlling the surface charge density will benefit a number of applications. As examples:

- *Prevention of electrostatic damage (ESD)*: The electrostatic charge produced by the triboelectric effect may cause sparks which can ignite flammable materials or vapors, interfering in the operation of electronics in the household, workplace, and societal infrastructures including public transportation, aircraft and spacecraft. It has been reported that related losses in the electronics industry are up to **US$5 billion**. (https://www.durablecorp.com/the-costs-of-esd-damage) Therefore, these industries would benefit from the ability to downregulate or decrease the triboelectric effect.
- *Power generation*: TENG is an emerging technology for low-frequency energy harvesting with demonstrated advantages of being lightweight, facile fabrication, high performance, and low cost [78]. It has been predicted that TENG and the resulting applications will be a **US$480 million market** by 2028 (https://www.idtechex.com/en/research-report/triboelectric-energy-harvesting-teng-2018-2028/577). As indicated by the TENG figure-of-merit (FOM) developed by the PI, TECD is the key parameter to maximize output performance [38]. Therefore, these applications would require that the triboelectric effect could be upregulated, maximized, or increased.

- *High-voltage applications*: For applications which require high-voltage input, such as the TENG-triggered electrospray for mass spectrometry (MS) demonstrated by the PI, quantitatively controlled charge generation is critical to achieving nanocoulomb level and ultrasensitive chemical analysis [79]. Similar research conducted by the PI includes field emission of electrons [78], and microplasma generation [80]. Here, the triboelectric effect should be tailored precisely according to the applications.
- *Self-powered wireless solution through tribophotonics*: Tribophotonics is coupling of triboelectricity as a self-powered solution and photonics as a wireless transmission solution, which was proposed in recent years [81]. The developed technologies under tribophotonics include tribo-induced EM-wave generation (TIEG), tribo-induced light propagation tuning (TILPT), tribo-induced electroluminescence (TIEL), and tribo-assisted spectrometry (TAS), which was detailed in Chapter 9. As induced by photon emission from CE, Li et al. also proposed CE-induced interface photon emission spectroscopy (CEIIPES), which can be considered a new type of TAS, and may be expanded as a new self-powered spectroscopy tool [36].

1.7 Summary

This chapter summarized the studies on CE mechanisms in recent years, as facilitated by the emerging field of TENG. Through experiments based on thermionic emission, intensive studies have been conducted on charge transfer mechanisms, with universal existence of electron transfer confirmed in CE through various studies. An electron-cloud-potential-well model was established, as key model for CE studies. In the meanwhile, the contributions from material transfer and ion transfer were studied in solid–solid interface and LSI CEs, respectively. The impacts of materials, environment, stress/strain, etc., were investigated, which greatly improved our understanding and provided charge modification tools for CE. It is expected that a more detailed CE mechanism will be revealed in the near future considering the intensive studies in recent years.

References

1 Wu, C., Wang, A.C., Ding, W. et al. (2019). Triboelectric nanogenerator: a foundation of the energy for the new era. *Adv. Energy Mater.* 9 (1): 1802906.
2 Hinchet, R., Yoon, H.-J., Ryu, H. et al. (2019). Transcutaneous ultrasound energy harvesting using capacitive triboelectric technology. *Science* 365 (6452): 491–494.
3 Zhu, G., Pan, C., Guo, W. et al. (2012). Triboelectric-generator-driven pulse electrodeposition for micropatterning. *Nano Lett.* 12 (9): 4960–4965.
4 Lebedev, M. and Akedo, J. (2002). What thickness of the piezoelectric layer with high breakdown voltage is required for the microactuator? *Jpn. J. Appl. Phys.* 41 (5B): 3344–3347.

5 Wang, J., Wu, C., Dai, Y. et al. (2017). Achieving ultrahigh triboelectric charge density for efficient energy harvesting. *Nat. Commun.* 8 (1): 88.
6 Lowell, J. and Rose-Innes, A.C. (2006). Contact electrification. *Adv. Phys.* 29 (6): 947–1023.
7 Liu, C. and Bard, A.J. (2008). Electrostatic electrochemistry at insulators. *Nat. Mater.* 7 (6): 505–509.
8 Liu, C.Y. and Bard, A.J. (2009). Chemical redox reactions induced by cryptoelectrons on a PMMA surface. *J. Am. Chem. Soc.* 131 (18): 6397–6401.
9 Liu, C.Y. and Bard, A.J. (2009). Electrons on dielectrics and contact electrification. *Chem. Phys. Lett.* 480 (4–6): 145–156.
10 Liu, C.-Y. and Bard, A.J. (2010). Electrostatic electrochemistry: nylon and polyethylene systems. *Chem. Phys. Lett.* 485 (1–3): 231–234.
11 Xu, C., Zi, Y., Wang, A.C. et al. (2018). On the electron-transfer mechanism in the contact-electrification effect. *Adv. Mater.* 30 (15): e1706790.
12 Xu, C., Zhang, B., Wang, A.C. et al. (2019). Effects of metal work function and contact potential difference on electron thermionic emission in contact electrification. *Adv. Funct. Mater.* 29 (29): 1903142.
13 Lin, S., Xu, L., Xu, C. et al. (2019). Electron transfer in nanoscale contact electrification: effect of temperature in the metal-dielectric case. *Adv. Mater.* 31 (17): e1808197.
14 Zhang, S.L., Xu, M., Zhang, C. et al. (2018). Rationally designed sea snake structure based triboelectric nanogenerators for effectively and efficiently harvesting ocean wave energy with minimized water screening effect. *Nano Energy* 48: 421–429.
15 Lin, S., Xu, L., Zhu, L. et al. (2019). Electron transfer in nanoscale contact electrification: photon excitation effect. *Adv. Mater.* 31 (27): e1901418.
16 Zhou, Y.S., Wang, S., Yang, Y. et al. (2014). Manipulating nanoscale contact electrification by an applied electric field. *Nano Lett.* 14 (3): 1567–1572.
17 Li, S., Zhou, Y., Zi, Y. et al. (2016). Excluding contact electrification in surface potential measurement using kelvin probe force microscopy. *ACS Nano* 10 (2): 2528–2535.
18 Wiles, J.A., Grzybowski, B.A., Winkleman, A., and Whitesides, G.M. (2003). A tool for studying contact electrification in systems comprising metals and insulating polymers. *Anal. Chem.* 75 (18): 4859–4867.
19 Thomas, S.W. 3rd, Vella, S.J., Kaufman, G.K., and Whitesides, G.M. (2008). Patterns of electrostatic charge and discharge in contact electrification. *Angew. Chem. Int. Ed.* 47 (35): 6654–6656.
20 McCarty, L.S. and Whitesides, G.M. (2008). Electrostatic charging due to separation of ions at interfaces: contact electrification of ionic electrets. *Angew. Chem. Int. Ed.* 47 (12): 2188–2207.
21 Thomas, S.W. 3rd, Vella, S.J., Dickey, M.D. et al. (2009). Controlling the kinetics of contact electrification with patterned surfaces. *J. Am. Chem. Soc.* 131 (25): 8746–8747.
22 Baytekin, H.T., Patashinski, A.Z., Branicki, M. et al. (2011). The mosaic of surface charge in contact electrification. *Science* 333 (6040): 308–312.

23 Baytekin, B., Baytekin, H.T., and Grzybowski, B.A. (2012). What really drives chemical reactions on contact charged surfaces? *J. Am. Chem. Soc.* 134 (17): 7223–7226.

24 Baytekin, H.T., Baytekin, B., Incorvati, J.T., and Grzybowski, B.A. (2012). Material transfer and polarity reversal in contact charging. *Angew. Chem. Int. Ed.* 51 (20): 4843–4847.

25 Siek, M., Adamkiewicz, W., Sobolev, Y.I., and Grzybowski, B.A. (2018). The influence of distant substrates on the outcome of contact electrification. *Angew. Chem. Int. Ed.* 57 (47): 15379–15383.

26 Pezzotti, G., Camara, C., Marin, E. et al. (2019). Physical chemistry insights into surface charge phenomena during frictional coupling in triboelectric X-ray sources. *J. Mater. Chem. C* 7 (25): 7708–7724.

27 Šutka, A., Mālnieks, K., Lapčinskis, L. et al. (2019). The role of intermolecular forces in contact electrification on polymer surfaces and triboelectric nanogenerators. *Energy Environ. Sci.* 12 (8): 2417–2421.

28 Ruckdeschel, F.R. and Hunter, L.P. (2008). Contact electrification between insulators: phenomenological aspects. *J. Appl. Phys.* 46 (10): 4416–4430.

29 Crowell, C.R. and Sze, S.M. (1966). Current transport in metal-semiconductor barriers. *Solid State Electron.* 9 (11): 1035–1048.

30 Ravinandan, M., Rao, P.K., and Rajagopal Reddy, V. (2009). Analysis of the current–voltage characteristics of the Pd/Au Schottky structure on n-type GaN in a wide temperature range. *Semicond. Sci. Technol.* 24 (3): 035004.

31 Crowell, C.R. (1965). The Richardson constant for thermionic emission in Schottky barrier diodes. *Solid State Electron.* 8 (4): 395–399.

32 Racko, J., Grmanová, A., and Breza, J. (1996). Extended thermionic emission-diffusion theory of charge transport through a Schottky diode. *Solid State Electron.* 39 (3): 391–397.

33 Xia, X., Wang, H., Guo, H. et al. (2020). On the material-dependent charge transfer mechanism of the contact electrification. *Nano Energy* 78: 105343.

34 Li, A., Liu, Y., and Szlufarska, I. (2014). Effects of interfacial bonding on friction and Wear at silica/silica interfaces. *Tribol. Lett.* 56 (3): 481–490.

35 Zhang, J., Rogers, F.J.M., Darwish, N. et al. (2019). Electrochemistry on tribocharged polymers is governed by the stability of surface charges rather than charging magnitude. *J. Am. Chem. Soc.* 141 (14): 5863–5870.

36 Li, D., Xu, C., Liao, Y. et al. (2021). Interface inter-atomic electron-transition induced photon emission in contact-electrification. *Sci. Adv.* 7 (39): eabj0349.

37 Xia, X., Wang, H., and Zi, Y. (2022). Field-assisted thermionic emission toward quantitative modeling of charge-transfer mechanisms in contact electrification. *SmartMat* 3 (4): 619–631.

38 Zi, Y.L., Niu, S.M., Wang, J. et al. (2015). Standards and figure-of-merits for quantifying the performance of triboelectric nanogenerators. *Nat. Commun.* 6: 8376.

39 Xu, W., Zheng, H., Liu, Y. et al. (2020). A droplet-based electricity generator with high instantaneous power density. *Nature* 578 (7795): 392–396.

40 Wu, H., Wang, Z., and Zi, Y. (2021). Multi-mode water-tube-based triboelectric nanogenerator designed for low-frequency energy harvesting with ultrahigh volumetric charge density. *Adv. Energy. Mater.* 11 (16): 2100038.

41 Jiang, P., Zhang, L., Guo, H. et al. (2019). Signal output of triboelectric nanogenerator at oil–water–solid multiphase interfaces and its application for dual-signal chemical sensing. *Adv. Mater.* 31 (39): 1902793.

42 Wang, P., Zhang, S., Zhang, L. et al. (2020). Non-contact and liquid–liquid interfacing triboelectric nanogenerator for self-powered water/liquid level sensing. *Nano Energy* 72: 104703.

43 Nie, J., Wang, Z., Ren, Z. et al. (2019). Power generation from the interaction of a liquid droplet and a liquid membrane. *Nat. Commun.* 10 (1): 2264.

44 Lin, S., Chen, X., and Wang, Z.L. (2022). Contact electrification at the liquid–solid interface. *Chem. Rev.* 122 (5): 5209–5232.

45 Magnussen, O.M. and Groß, A. (2019). Toward an atomic-scale understanding of electrochemical Interface structure and dynamics. *J. Am. Chem. Soc.* 141 (12): 4777–4790.

46 Zaera, F. (2012). Probing liquid/solid interfaces at the molecular level. *Chem. Rev.* 112 (5): 2920–2986.

47 Lee, S.H., Nedrygailov, I.I., Oh, S., and Park, J.Y. (2018). Hot electron flux at solid–liquid interfaces probed with Pt/Si catalytic nanodiodes: effects of pH during decomposition of hydrogen peroxide. *Catal. Today* 303: 282–288.

48 Tao, F. and Crozier, P.A. (2016). Atomic-scale observations of catalyst structures under reaction conditions and during catalysis. *Chem. Rev.* 116 (6): 3487–3539.

49 Wang, J., Wang, H., Li, X., and Zi, Y. (2019). Self-powered electrowetting optical switch driven by a triboelectric nanogenerator for wireless sensing. *Nano Energy* 66: 104140.

50 Li, X., Tian, H., Shao, J. et al. (2016). Decreasing the saturated contact angle in electrowetting-on-dielectrics by controlling the charge trapping at liquid–solid interfaces. *Adv. Funct. Mater.* 26 (18): 2994–3002.

51 Helmholtz, H. (1853). Ueber einige Gesetze der Vertheilung elektrischer Ströme in körperlichen Leitern mit Anwendung auf die thierisch-elektrischen Versuche. *Ann. Phys.* 165 (6): 211–233.

52 Stern, O. (1924). The theory of the electric double layer. *Electrochemistry* 30: 508.

53 Nie, J., Ren, Z., Xu, L. et al. (2020). Probing contact-electrification-induced electron and ion transfers at a liquid–solid interface. *Adv. Mater.* 32 (2): 1905696.

54 Lin, S., Xu, L., Chi Wang, A., and Wang, Z.L. (2020). Quantifying electron-transfer in liquid-solid contact electrification and the formation of electric double-layer. *Nat. Commun.* 11 (1): 399.

55 von Burg, K. and Delahay, P. (1981). Photoelectron emission spectroscopy of inorganic anions in aqueous solution. *Chem. Phys. Lett.* 78 (2): 287–290.

56 Takakuwa, Y., Niwano, M., Nogawa, M. et al. (1989). Photon-stimulated desorption of H+ ions from oxidized Si(111) surfaces. *Jpn. J. Appl. Phys.* 28 (12R): 2581.

57 Zhan, F., Wang, A.C., Xu, L. et al. (2020). Electron transfer as a liquid droplet contacting a polymer surface. *ACS Nano* 14 (12): 17565–17573.

58 Wang, Z.L. and Wang, A.C. (2019). On the origin of contact-electrification. *Mater. Today* 30: 34–51.

59 Wang, A.C., Zhang, B., Xu, C. et al. (2020). Unraveling temperature-dependent contact electrification between sliding-mode triboelectric pairs. *Adv. Funct. Mater.* 30 (12): 1909384.

60 Xu, C., Wang, A.C., Zou, H. et al. (2018). Raising the working temperature of a triboelectric nanogenerator by quenching down electron thermionic emission in contact-electrification. *Adv. Mater.* 30 (38): 1803968.

61 Zhu, Y., Lin, S., Gao, W. et al. (2021). Reversal of triboelectric charges on sol–gel oxide films annealed at different temperatures. *Appl. Phys. Lett.* 118 (24): 243902.

62 Lin, S., Xu, L., Xu, C. et al. (2019). Electron transfer in nanoscale contact electrification: effect of temperature in the metal–dielectric case. *Adv. Mater.* 31 (17): 1808197.

63 Zou, H., Guo, L., Xue, H. et al. (2020). Quantifying and understanding the triboelectric series of inorganic non-metallic materials. *Nat. Commun.* 11 (1): 2093.

64 Zou, H., Zhang, Y., Guo, L. et al. (2019). Quantifying the triboelectric series. *Nat. Commun.* 10 (1): 1427.

65 Wang, S., Zi, Y., Zhou, Y.S. et al. (2016). Molecular surface functionalization to enhance the power output of triboelectric nanogenerators. *J. Mater. Chem. A* 4 (10): 3728–3734.

66 Zhang, X.-S., Han, M.-D., Wang, R.-X. et al. (2014). High-performance triboelectric nanogenerator with enhanced energy density based on single-step fluorocarbon plasma treatment. *Nano Energy* 4: 123–131.

67 Wang, J., Li, S., Yi, F. et al. (2016). Sustainably powering wearable electronics solely by biomechanical energy. *Nat. Commun.* 7 (1): 12744.

68 Zhong, J., Zhong, Q., Fan, F. et al. (2013). Finger typing driven triboelectric nanogenerator and its use for instantaneously lighting up LEDs. *Nano Energy* 2 (4): 491–497.

69 Wang, J., Wen, Z., Zi, Y. et al. (2016). All-plastic-materials based self-charging power system composed of triboelectric nanogenerators and supercapacitors. *Adv. Funct. Mater.* 26 (7): 1070–1076.

70 Cui, N., Gu, L., Lei, Y. et al. (2016). Dynamic behavior of the triboelectric charges and structural optimization of the friction layer for a triboelectric nanogenerator. *ACS Nano* 10 (6): 6131–6138.

71 Li, S., Nie, J., Shi, Y. et al. (2020). Contributions of different functional groups to contact electrification of polymers. *Adv. Mater.* 32 (25): e2001307.

72 Xu, G., Guan, D., Fu, J. et al. (2022). Density of surface states: another key contributing factor in triboelectric charge generation. *ACS Appl. Mater. Interfaces* 14 (4): 5355–5362.

73 Xu, C., Zhang, B., Wang, A.C. et al. (2019). Contact-electrification between two identical materials: curvature effect. *ACS Nano* 13 (2): 2034–2041.

74 Lin, S., Zheng, M., Xu, L. et al. (2022). Electron transfer driven by tip-induced flexoelectricity in contact electrification. *J. Phys. D. Appl. Phys.* 55 (31): 315502.

75 Liu, Z., Li, S., Lin, S. et al. (2022). Crystallization-induced shift in a triboelectric series and even polarity reversal for elastic triboelectric materials. *Nano Lett.* 22 (10): 4074–4082.

76 Tao, X., Nie, J., Li, S. et al. (2021). Effect of photo-excitation on contact electrification at liquid–solid interface. *ACS Nano* 15 (6): 10609–10617.

77 Lin, S., Xu, L., Tang, W. et al. (2019). Electron transfer in nano-scale contact electrification: atmosphere effect on the surface states of dielectrics. *Nano Energy* 65: 103956.

78 Wang, Z.L., Lin, L., Chen, J. et al. (2016). *Triboelectric Nanogenerators*. Springer.

79 Li, A., Zi, Y., Guo, H. et al. (2017). Triboelectric nanogenerators for sensitive nano-coulomb molecular mass spectrometry. *Nat. Nanotechnol.* 12 (5): 481.

80 Cheng, J., Ding, W., Zi, Y. et al. (2018). Triboelectric microplasma powered by mechanical stimuli. *Nat. Commun.* 9 (1): 3733.

81 Wang, H., Xia, X., Fu, J. et al. (2023). A general self-powered wireless sensing solution based on triboelectric-discharge effect. *Nano Energy* 105: 107982.